# A 2.3-mW 11-cm Range Bootstrapped and Correlated-Double-Sampling Three-Dimensional Touch Sensing Circuit for Mobile Devices

Li Du, Yan Zhang, Chun-Chen Liu, Adrian Tang, *Senior Member, IEEE*, Frank Hsiao, and Mau-Chung Frank Chang, *Fellow, IEEE*

***Abstract*—This brief discusses an oscillator-based capacitive 3-D touch-sensing circuit for mobile devices. The proposed 3-D touch sensor uses correlated double sampling to achieve a high sensing resolution in the Z-direction and employs bootstrapping circuitry to reduce the mobile screen's interchannel-coupling effects. Additionally, to reduce chip area and assembly, the sensing oscillator is implemented with inverter-based active resonators instead of using either on- or off-chip inductors. The prototyped 3-D touch sensor is fabricated using 65-nm CMOS process technology and consumes an area of 2 mm$^2$, with a 2.3-mW power consumption from a 1-V power supply. Measured together with a 3.4″ HTC standard mobile screen, the sensor achieves an 11-cm Z-direction sensing range with a 1-cm resolution, demonstrating the potential implementation of 3-D finger position sensing in a mobile device.**

***Index Terms*—Bootstrapping, correlated double sampling (CDS), interchannel coupling, mobile device, touch screen, 3-D.**

## I. Introduction

Touch sensing is one of the major modern human/machine interfaces and has been widely implemented in various display products (e.g., smartphones, tablets, and TV) as its user-friendly interface, low power, and lightweight assembly are well suited to these applications. Traditional touch screens require the user's finger to contact the screen in order to induce a detectable level of finger capacitance. The required physical contact inherent of the technology creates several disadvantages, including unresponsiveness due to wet fingers, and unavoidable fingerprint residue on the screen surface. Beyond these basic limitations, the emerging wearable device market creates additional challenges when compared with traditional mobiles as they offer much smaller display sizes [1], further exacerbating sensing resolution and sensitivity as finger capacitances are reduced.

Recently, significant progress has been made in developing 3-D touch sensing technology, which can detect the finger position, and even hand gestures, remotely when the finger is hovering over the screen. Hu *et al.* [2] report sensing users' gestures using capacitive sensing in front of the display with a customized touch electrode to remove noise and coupling effects. In [3], up to 10 cm of $z$-axis distance was achieved by using a large electrode to generate more finger capacitance. Among these reported works, employing large customized electrodes on the display is a common approach and plays a critical role in mitigating the channel-coupling effects of the touch panel and increasing the sensed finger capacitance. However, due to the limited form factors and required 2-D resolution, it is not possible to customize the electrodes in mobile devices in the same fashion as in large displays.

To infuse this technology into volume- and power-constrained mobile devices whose touch panel size and electrode pattern are fixed, a paradigm shift in the touch-sensor system design is essential to sense the very small changes in finger capacitance coupled with the challenge of much smaller size and strongly intercoupled electrodes. In addition, any successful 3-D sensing solution for mobile devices must consume very low power and small silicon area in order to be compatible with the limited battery and space resources. In this brief, a 2.3-mW 11-cm range bootstrapped and correlated double sampling (CDS) (BCDS) 3-D touch sensor specifically for mobile devices is reported in detail (originally summarized in [4]). This brief is organized as follows. In Section II, the BCDS system concept architecture is introduced. In Section III, we present the channel load trimming calibration used in our system. In Section IV, the circuit implementation of the active sensing oscillator is explained. Section V describes our measurement results. Finally, we summarize the proposed touch sensor in Section VI.

## II. System Architecture

Fig. 1 shows the overall BCDS system architecture. The system contains an oscillator-based CDS module with a trimming capacitor array at the oscillator input to enable high-resolution self-capacitance sensing and also contains bootstrapping circuitry to mitigate the channel-coupling effects.

### A. Oscillator-Based CDS

The channel's load capacitance change is measured through an inverter-based LC oscillator whose frequency is monitored via a digital counter with a specific integration time (observing time window). Unlike traditional oscillator-based capacitive

Manuscript received November 21, 2015; accepted April 5, 2016. Date of publication April 14, 2016; date of current version December 22, 2016. This brief was recommended by Associate Editor M. Tse.

The authors are with the Department of Electrical Engineering, University of California, Los Angeles, CA 90095 USA (e-mail: dl1989113@ucla.edu).

Color versions of one or more of the figures in this brief are available online at http://ieeexplore.ieee.org.

Digital Object Identifier 10.1109/TCSII.2016.2554218

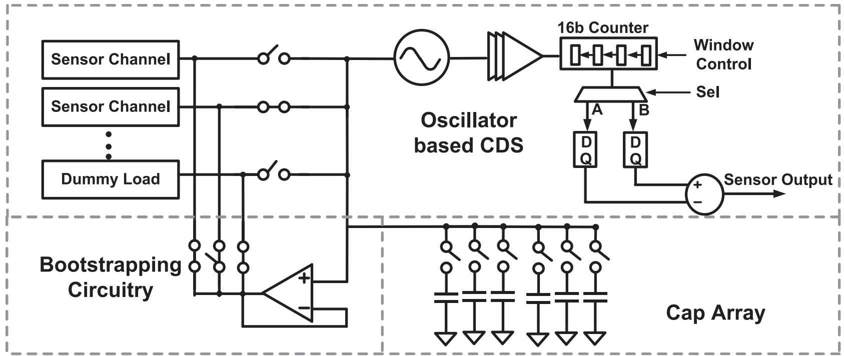


Fig. 1. Overall BCDS system architecture.

sensing, the integrated counter value will be directly equated with the channel's load capacitance. The CDS sensing uses a dummy load to cancel the channel's intrinsic self-capacitance and outputs only the sensed finger-induced capacitance of the channel. During each measurement cycle, the oscillator is first connected to the desired input sensor channel for a given integration time and then connected to a dummy load with similar capacitance for the same integration time. During each integration window, a digital counter records the number of periods that the oscillator completes, which reflects the oscillation frequency. Since the finger-induced capacitance is very small compared with the channel intrinsic self-capacitance, the output counter code difference is directly proportional to the sensed finger capacitance derived as

$$C_{\text{finger}} = \Delta C = \frac{1}{4\pi^2 (f-\Delta f)^2 L} - \frac{1}{4\pi^2 f^2 L} \approx \frac{\Delta f}{2\pi^2 f^3 L} \quad (1)$$

where $f$ corresponds to the oscillation frequency, and $L$ is the oscillator's inductor value. In addition, if the active channel's intrinsic capacitance and dummy channel load are well matched, any low-frequency noise (i.e., oscillator's flicker noise) will be shown in the counter value of both the active channel case and the dummy channel case. Based on outputting the counter's difference between the input channel and dummy channel, the system will cancel most of the low-frequency noise through generating a zero at the DC in its frequency transfer function. The equivalent frequency transfer function of the CDS integration can be derived as

$$\begin{aligned} Y(t) &= \int_{t-t_0}^{t} X(t) - \int_{t}^{t+t_0} X(t) \\ &= \int_{-\infty}^{t} 2X(t) - X(t-t_0) - X(t+t_0) \quad (2) \\ H(f) &= \frac{F(Y(t))}{F(X(t))} = \frac{1}{j2\pi f}(2 - e^{j2\pi t_0 f} - e^{-j2\pi t_0 f}) \\ &= \frac{4\sin(\pi t_0 f)^2}{j2\pi f} = -2j\text{sinc}(\pi t_0 f) t_0 \sin(\pi t_0 f) \quad (3) \end{aligned}$$

where $t_0$ is the integration window time. When $f$ is close to DC, the transfer function can be approximated as (4), showing a zero at the DC

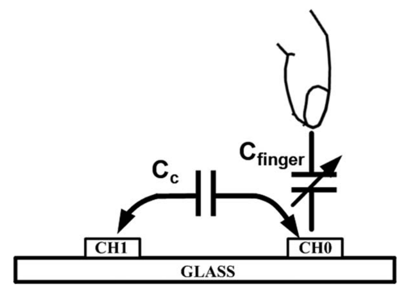


Fig. 2. Channel-coupling effect in small touch screens (when $C_c \gg C_{\text{finger}}$, both CH0 and CH1 will show an equal response).

$$H(f) = -2\pi j \text{sinc}(\pi t_0 f) t_0^2 f. \quad (4)$$

In (5) and (6), we derive the transfer function for a system without correlated sampling, showing that low-frequency noise exhibits a large gain near DC, limiting the system's sensitivity to small changes of capacitance

$$\begin{aligned} Y(t) &= \int_{t-t_0}^{t} X(t) = \int_{-\infty}^{t} X(t) - X(t-t_0) \quad (5) \\ H(f) &= \frac{F(Y(t))}{F(X(t))} = \frac{1}{j2\pi f}(1 - e^{j2\pi f t_0}) \\ &= \text{sinc}(\pi t_0 f) t_0 e^{-j\pi f t_0}. \quad (6) \end{aligned}$$

### B. Bootstrapping Circuitry

In addition to the challenges of detecting the small finger capacitance change in 3-D sensing compared with 2-D sensing, the large channel-to-channel coupling capacitance (typically in the range of 20–100 pF for a mobile screen [5]) also limits the system sensitivity, causing a resolution degradation in the horizontal direction during the channel scanning process. This difficulty is illustrated in Fig. 2.

When the finger is approaching Channel 0 (CH0), a femtofarad-level finger capacitance $C_{\text{finger}}$ is induced onto CH0. Ideally, the system should only see the induced capacitance experienced as an increase in CH0's self-capacitance. However, if the interchannel capacitor $C_c$ is much larger than $C_{\text{finger}}$, the finger capacitance will couple to CH1 through $C_c$, providing

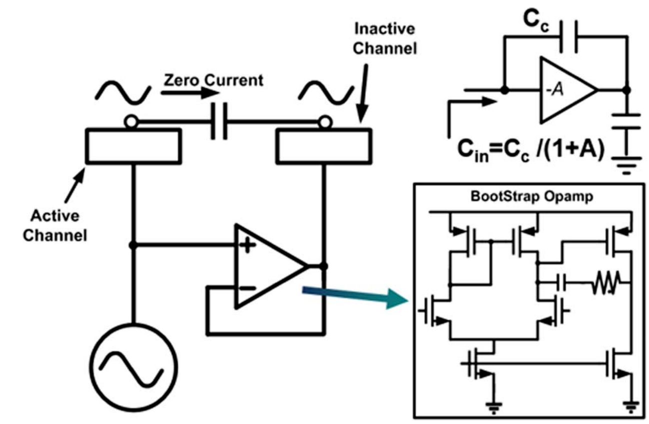


Fig. 3. Introduced bootstrapped circuitry showing the suppression of the coupling capacitance through the tracking amplifier.

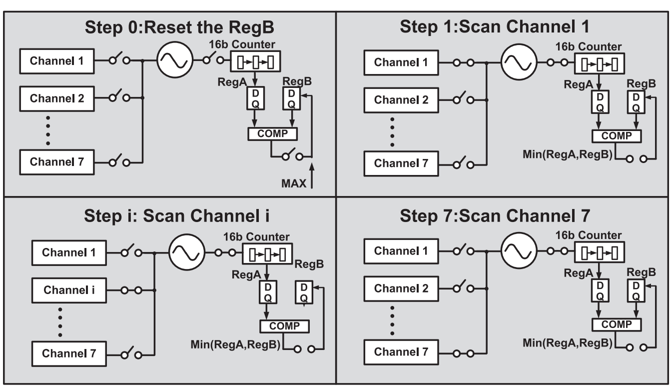


Fig. 4. Procedure for determining the maximum channel load.

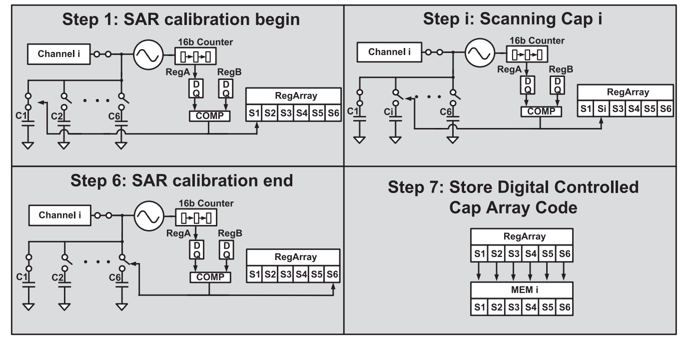


Fig. 5. Procedure of calibrating Channel 1's load using a specific absorption rate algorithm.

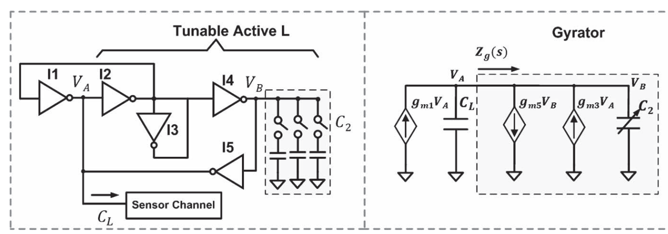


(a) (b)

Fig. 6. (a) Simplified schematic of the inverter-based active resonator and (b) its corresponding small signal mode.

an equal channel response between CH0 and CH1, which will cause a false horizontal position detection. To overcome this, bootstrapping circuitry is introduced between channels to eliminate the coupling capacitance, as depicted in Fig. 3. As the electrode array is scanned, a unity-gain amplifier is used to sense the time-domain voltage of the currently active channel and replicate it on the remaining inactive channels to nullify the coupling capacitance by enforcing equal potential across the interchannel coupling capacitors. In this case, the coupling capacitance seen from the active channel is suppressed.

## III. Calibration of the Channel Load

As discussed in Section II, in order to use the CDS to cancel noise, an equal electrical load capacitance among all channels, including the dummy channel, is necessary. To achieve this, a two-step channel load trimming calibration scheme is employed. Fig. 4 shows the first step of the calibration sequence that searches for the maximum load capacitance channel. The system scans each channel and monitors the counter value (equated to oscillator frequency) for a fixed time. In each scan, the counter's output result stored in RegA will be compared with RegB's value. If it is smaller than RegB's value, it will replace the current RegB's value. After the scanning, the maximum channel's load capacitance value will be stored in RegB as the reference load value, which is used to calibrate the remaining channels' load capacitance.

During the second step of the calibration, each channel will be calibrated individually by using a switched capacitor array to trim the channel capacitance to closely match the reference load value. This is achieved by successively approximating the readout counter value to be as close to the RegB value through a 6-b binary capacitor array, as shown in Fig. 5. After the calibration sequence, the capacitor array's value will be stored in the memory and will be loaded during normal scanning to trim each channel's load to match the reference. In normal scanning, if no finger is approaching the sensor, the CDS output will remain close to zero, whereas if a finger is approaching, the counter will output a positive number.

## IV. Circuit Implementation of the Oscillator

Fig. 6(a) shows the design of the CDS oscillator for the proposed BCDS sensing system. The nature of self-capacitance touch sensing prefers a single-ended capacitance-modulation action as opposed to a differential implementation. In addition, the limited gain and bandwidth of the bootstrapping amplifier requires a sinusoidal waveform instead of a square wave to avoid performance deterioration due to poor waveform replication at higher harmonics. Unlike a traditional LC single-ended oscillator with a large on-chip or off-chip passive element (such as the off-chip inductor used in [2]), the BCDS sensor employs an inverter-based active resonator similar to that reported in [6]. The right four inverters I2, I3, I4, and I5 construct a gyrator to form an equivalent active inductor, while the left inverter (I1) serves as a negative resistor to provide energy to the resonator. The equivalent small signal mode of the circuit can be derived

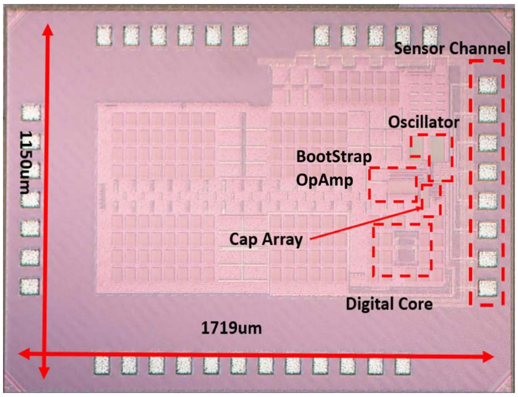


Fig. 7. Die photograph of the BCDS sensor with major blocks identified.

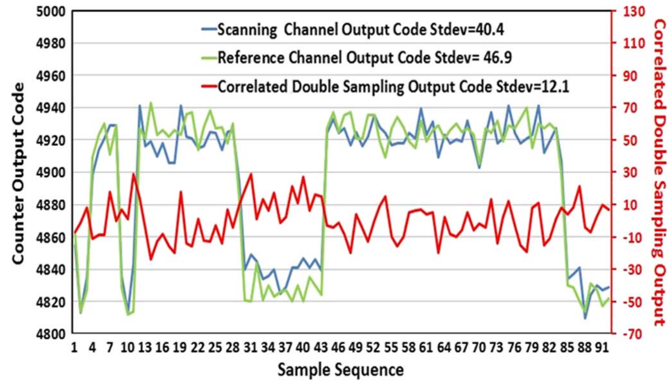


Fig. 8. Measurement of the counter output for the reference (dummy load) channel and an actively scanned channel showing that the oscillator is correlated between both conditions.

as Fig. 6(b), with a corresponding oscillating frequency derived as (9)

$$Z_g(s) = \frac{V_A}{g_{ms}V_B} = \frac{sC_2}{g_{ms}g_{ms}} \tag{7}$$

$$L_e = \frac{C_2}{g_{m5}g_{m3}} \tag{8}$$

$$f = \frac{1}{2\pi\sqrt{L_eC_L}} = \frac{1}{2\pi\sqrt{L_eC_L}} = \frac{1}{2\pi}\sqrt{g_{m5}g_{m3}/C_LC_2} \tag{9}$$

where $Z_g(s)$ is the Laplace transform of the input impedance of the gyrator, $C_L$ is the channel load capacitance, and $C_2$ is a tunable capacitor array to alter the active inductor value so that the oscillator frequency can be varied.

To further ease the bootstrapping amplifier's design, reduce the power consumption, and improve the oscillator's linearity, diode clamps are paired with each inverter to reduce the voltage swing of the oscillator.

## V. Experimental Results

The proposed BCDS sensing circuit was implemented with seven sensing channels and fabricated in a 65-nm CMOS process, occupying an area of 2 $mm^2$, as shown in Fig. 7. The whole chip consumes 2.3 mW in normal operation.

To evaluate the effectiveness of the BCDS sensor on the 3-D mobile touch screen, we connect the prototyped sensor with a standard HTC 3.4″ mobile touch screen (channel number: X = 16 and Y = 10). The first measurement performed validates the effectiveness of double sampling operation. We first record the sensor's counter output of both the reference (dummy load) and active channel case independently, plot their values, and compute their standard deviation. Then, we perform the subtraction operation to produce the CDS output. Fig. 8 shows the counter output code for both the active and reference channel as well as the final CDS output. Based on this result, we see a high level of correlation between the active and reference channels, providing a 10.5-dB reduction of the counter output's standard deviation.

Second, to characterize the sensitivity of the BCDS sensor to the finger height position, a finger is moved above the centered Y channel. The measured BCDS output code versus the finger height, together with the setup, is shown in Fig. 9. Based on the

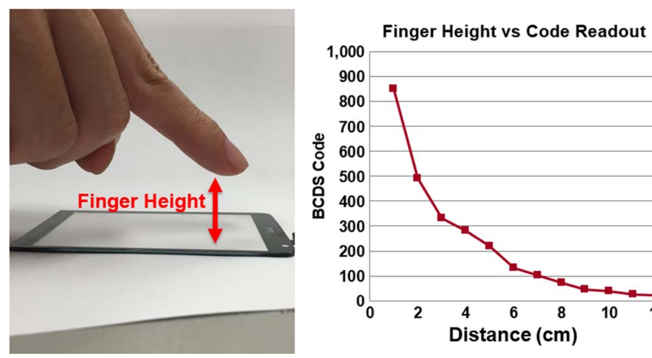


Fig. 9. BCDS output code versus finger height.

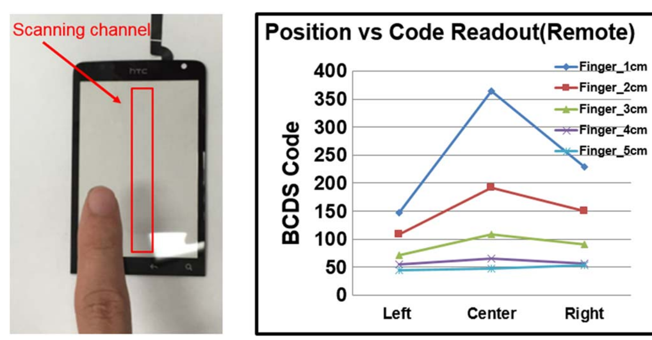


Fig. 10. BCDS output code versus finger position for different finger heights.

output codes' difference among various finger heights and the noise of the system (the output code standard deviation), a final Z-direction resolution of 10 mm is computed for a maximum finger range of 11 cm.

Finally, to verify the effectiveness of the bootstrapping technique for eliminating interchannel coupling, the active channel is connected to a Y channel located in the center of the screen while a finger is swept from left to right at different heights. The measured BCDS response is shown in Fig. 10. As shown, when the finger is close to the screen ($<$ 3-cm height), the bootstrapping circuitry provides sufficient coupling isolation, resulting in an 8-dB BCDS output code difference with the finger in different X positions. When the finger is above a certain height ($>$ 4 cm), the reduction of the induced finger capacitance, along with the limited gain of the bootstrapping

TABLE I
PERFORMANCE SUMMARY AND COMPARISON

| | ISSCC12 [7] | ISSCC14 [2] | MGC3130 [3] | This Work |
|---|---|---|---|---|
| Sensing Type | 2D Mobile | 3D Large Screen | 3D Large Screen | 3D Mobile |
| External Component Required | No | Yes(33uH inductor) | No | No |
| Electrode Spacing | X | 100mm | 48mm | 4.8mm (Standard HTC3.4“ Screen) |
| Normalized Sensing Height (Height/Panel Area) | 0 | 0.018cm-1 (30cm/(40cm×40cm)) | 0.1cm-1 (15cm/(14.8cm×9.9cm)) | 0.32cm-1 (11cm/(7.2cm×4.8cm)) |
| Height Resolution | X | 10mm (Screen Size: 40cm×40cm) | X | 10mm (Screen size:7.2cm×4.8cm) |
| SNR | 35dB@0cm | 50dB@5cm 30dB@16cm | X | 36dB@1cm 25dB@5cm |
| Power Consumption | 10.6mW | 19mW | 150mW | 2.3mW |
| Die Area | 6.87mm$^2$ | 4.2mm$^2$ | X | 2mm$^2$ |
| Technology | 1.5/5.5/30V 90nmLDI | 1.2/2.5V 130nm CMOS | X | 1V 65nm CMOS |

amplifier, overcomes the cancellation, and the BCDS can no longer support the X position differentiation.

Table I compares the performance of the BCDS touch sensor with several other state-of-the-art touch sensors [2], [3], [7]. The proposed BCDS provides comparable Z range and resolution to the other reported 3-D contactless touch sensors. Note that the works in [3], [4], and [8] are intended for much larger TV displays where the electrode spacing is much larger and for a substantially larger electrode area to attract more finger capacitance. To provide a fair comparison between our work and the reported results, we have normalized the sensing height over the panel size as listed in the fifth row (Height Resolution) of Table I. The demonstrated BCDS prototype sensor provides a factor of 3 to 17X improvement in normalized sensing height over that of prior arts, making it more suitable for mobile device touch screens. A synchronous demo of the finger position capture using this BCDS sensor is shown in [8].

## VI. CONCLUSION

A new 3-D touch sensor specifically for mobile devices has been presented. The proposed touch sensor uses CDS to boost vertical sensing range and bootstrapping circuitry to eliminate the large interchannel-coupling effects of mobile screens. The sensor employs an on-chip inductorless resonator to reduce production and assembly costs through reduced I/O and chip area. Compared with other 3-D touch sensors targeting the large display market, our demonstrated BCDS sensor is shown to be more suitable for implementing 3-D touch sensing in mobile devices with tightly spaced, more resistive, and strongly intercoupled electrodes and smaller display sizes.

## ACKNOWLEDGMENT

The authors would like to thank Taiwan Semiconductor Manufacturing Company for the foundry support and Wintek Corporation for providing a touch-screen sample.

## REFERENCES

[1] P. Koundinya *et al.*, “Multi resolution touch panel with built-in fingerprint sensing support,” in *Proc. DATE Conf. Exhib.*, 2014, Mar. 2014, pp. 1–6.
[2] Y. Z. Hu *et al.*, “3D gesture-sensing system for interactive displays based on extended-range capacitive sensing,” in *Proc. IEEE Int. Solid-State Circuits Conf.*, Feb. 2014, pp. 212–213.
[3] Microchip Technology, Inc., Chandler, AZ, USA, MGC3130 Data Sheet. [Online]. Available: https://www.microchip.com/wwwproducts/en/mgc3130
[4] L. Du *et al.*, “A 2.3 mW 11 cm range bootstrapped and correlated double sampling (BCDS) 3D touch sensor for mobile devices,” in *Proc. IEEE Int. Solid-State Circuits Conf.*, Feb. 22–26, 2015, pp. 122–123.
[5] T. O’Connor, “mTouch projected capacitive touch screen sensing theory of operation,” Microchip Technology, Inc., Chandler, AZ, USA. [Online]. Available: http://ww1.microchip.com/downloads/en/DeviceDoc/93064A.pdf
[6] H. Barthelemy, S. Bourdel, J. Gaubert, and M. Battista, “CMOS inverters based high frequency voltage controlled sinusoidal oscillator,” in *Proc. IEEE Int. Conf. Electron., Circuits Syst.*, Dec. 2007, pp. 490–493.
[7] K.-D. Kim *et al.*, “A capacitive touch controller robust to display noise for ultrathin touch screen displays,” in *Proc. IEEE Int. Solid-State Circuits Conf.*, Feb. 2012, pp. 116–117.
[8] Airtouch demo with software interface. [Online]. Available: youtu.be/x0xgKJwmGWU